# Factor influencing point load tests on concrete

**Rahmat Madandoust[a], Zeynab Fallah Zarjoo Bazkiyaei[a] Mostafa Kazemi[a]**

[a]Department of Civil Engineering, University of Guilan, P.O. Box 3756,Rasht, Iran

**Corresponding Author:** Rahmat Madandoust

**E-mail:** rmadandoust@guilan.ac.ir

**Tel**: +98 9113314970

**Fax**: +98 1333690271

**Abstract**

The main purpose of this paper is to predict the in-situ compressive strength of concrete by means of point load strength test (PLT) as a partially destructive test method. This test method is examined by extracting core specimen from concrete blocks and applying two point loads to the lateral surface of the core specimen. The failure in the core specimen is occurred in the direction of applying load where most normal stresses are tensile, while some compressive stresses are generated in the contact surface of load cell with the core specimen. In this study, point load index (PLI) in which a force is divided by the square of the distance between the platen points and cube compressive strength (CS) was determined under wet and dry curing conditions at the ages of 7, 14, 28 and 42 days. The effects of various parameters such as core diameter and length to diameter (L/D) ratio were considered experimentally and numerically by means of finite element method using ABAQUS software. A three dimensional finite element model (FEM) was constructed to study the stress magnitude and stress distribution at the failure surface. The results showed that the PLI in wet curing conditions were about 12 % higher than those in dry curing conditions. In addition, The PLI increased particularly steep when the L/D ratio is less than 1, while then becomes less steep when the L/D ratio is between 1 and 1.8. Meanwhile, it seems that there is no significant difference among PLI values for the ratios of L/D more than 1.8.

**Keywords:** Point load strength test, Concrete rupture, Concrete cores, Compressive strength, Finite element analysis.

## 1. Introduction

There has always been a need for some test methods to measure the in-situ concrete strength for evaluation of the existing conditions. One of these test methods is the point load strength test (PLT) which is known as a partially destructive test to examine the in-situ concrete compressive strength of structural members. Similar to Brazilian splitting test, used for estimating indirect tensile strength of concrete, which consists of applying a diametral compressive load along the length of a cylindrical concrete specimen at a rate that is within a prescribed range until failure occurs, the PLT is based on breaking a concrete specimen which is subjected to an increasingly concentrated point load, applied through a pair of conical platens. However, unlike Brazilian tensile splitting test, the PLT offers a practical alternative to the compressive testing of cores (Robins, 1980). Some advantages of this simple test are that trimming and capping are not required and that the testing forces are lower, thus permitting the use of small portable equipment on site at a reduced unit cost (Bungey et al., 2006). In addition, the PLT is associated with simplicity of sample preparation and testing on the site with portable apparatus. Broch and franklin (1972) provided more detailed description about this test and the international society for Rock Mechanics Committee (ISRM, 2009) has considered the PLT as a recommended test. Robins (1980) first suggested the idea of PLT for concrete samples. He claimed that the testing variability is comparable to conventional core compressive strength using this approach. Zacoeb et al. (2007) found that the point load index (PLI) for a core specimen with a diameter of 50 mm has a good correlation with concrete core strength. Zacoeb and Ishibashi (2009) obtained PLI results using two L/D ratios of core specimen. They evaluated the reliability of PLT results for each core specimen and suggested a new geometric correction factor. They used finite element analysis software "ANSYS" for analyzing internal stress of core specimen during the PLT.

They also revealed that the reduction in L/D ratio from 2 to 1.5 leads to tensile stress progress in central axis direction. They recommended core drilled diameter of 50 mm and L/D ratio of 2 are better than core diameter of 35 mm and L/D ratio of 1.5 for in-situ concrete strength estimation by using PLT.

The relationship between PLI and compressive strength (CS) were studied by Selçuk and Gökçe (2015) using regression analysis. To study the stress distribution within the specimen in diametral PLT, some analytical methods have been developed. Concerning this, a solution has been presented by Al-Derbi and Freitas (1999), based on the concept of the Boussinesq equation, as suggested by Wijk (1980). Chau and Wei (2001) presented an exact analytic solution for a finite isotropic circular cylinder subjected to the diametral PLT. Russell and Wood (2009) estimated the mobilization of failure according to a recently established multriaxial failure criterion for brittle materials such as rocks and concrete by means of analysis of the stress state in spherical elastic samples resulting from diametral loading applied over a small contact area around the nominal point of contact. Nowadays, finite element model (FEM) is widely used to study and describe the nonlinear behavior of structures and the results, obtained from these analyses, can be cited with a high confidence level. As shown by Wang (2005), theoretical investigations and extension of numerical methods on PLT are rapidly increasing and including the latest research by the comprehensive research, in which a field test was modeled by ABAQUS software.

Although many researches have been performed on the relationship between CS and PLI for different rock types, a limited number of studies have been conducted by researchers on the effects of shape and size of concrete specimen on PLI. Therefore, the main objective of this paper is to present an experimental investigation on the effects of curing conditions, concrete age, core diameter and strength level on the CS and PLI. The correlations between cube CS and PLI on small core specimens were also established. Furthermore, an analytical study based on finite element analysis was performed to verify the result of the experimental data. FEM has been used to predict the behavior of concrete core under monotonic loading. The effect of specimen size on the PLI was studied numerically on specimens with L/D ratios ranging from 0.5 to 3. The load-displacement responses and the stress distributions were obtained from this numerical simulation and compared with laboratory specimen results. The stress distribution along the line of loading was determined and the relationship between PLI and maximum tensile strength in specimen was examined.

## 2. Experimental Program

### 2.1. Materials and mixture proportion

Type II portland cement, produced in Hegmatan factory, was used with specific gravity of 3.15 gr/cm$^3$ and Blaine fineness of 2900 gr/cm$^3$. This study investigated the concrete strength in two different levels. For this purpose, two W/B ratios such as 0.63 and 0.45 were considered. In W/B=0.45, Silica fume (SF), provided from Ferro Alloy Azna factory, as a partial replacement of cement at 10% was added to enhance their strength. The chemical compositions of cement and SF are given in Table 1. The fine aggregate was washed river sand with a specific gravity of 2.63. The coarse aggregate with a specific gravity of 2.65 was crushed limestone with maximum size of 12.5 mm. A polycarboxylic-ether type superplasticizer (SP) was utilized to achieve the desired workability in concrete with a low W/B ratio. Proportions of the concrete mixes are given in Table 2. In this table, M1 refers to concrete without SF and M2 is defined as the concrete mixture with a replacement level of 10 % SF.

### 2.2. Specimen preparation

The CS of various concrete mixes was measured using 100 mm cube specimens in accordance with BS 1881-108 where the rate of loading was 0.25 MPa/s. For the PLT, four concrete slabs were cast using 900×900×150 mm as shown in Fig. 1. The specimens were demoulded after 24 hours and then were cured either wet or dry curing conditions until the time of testing. The cast specimens were covered with polyurethane sheet and damped cloth in a 22±2 °C chamber and were left in the casting room for 1 day according to ASTM C192. Following removal from the mold, half of the specimens were transferred to a moist curing room at 100 % relative humidity with temperature of about 20 °C; the other half of which were covered with polyurethane sheet set for about three days, thereby being exposed to dry at 20 °C.

### 2.3. Test methods

According to the most of the standards, core samples should be drilled not earlier than 7 days since the cores may be considerably damaged by drilling. The cores with diameters of 50 and 70 mm were removed from the slabs by drilling in the direction of concrete placement. The CS test and PLT results are the average of at least three and six specimens, respectively. Since Zacoeb and Ishibashi (2009) recommended to select as specimen with L/D ratio of 2 for in-situ concrete strength estimation by using PLT, in this study, specimens with L/D ratio of 2 were evaluated for both concrete mix designs (M1 and M2) at the ages of 7, 14, 28 and 42 days under wet and dry curing conditions. To assess the effects of various L/D ratios on the results of PLT, other specimens with L/D ratios of 0.5, 1 and 3 were tested on mix M1 under wet curing conditions at the age of 28 days and compared with each other. The PLT equipment consists of a loading set-up, loading pump, gauges, two conical platens and a scale that measures distance between two conical platens. In PLT, concrete cores are loaded between two conical steel platens until failure occurs (Fig. 2). The loading rate was considered to be 0.01 in/min similar to the assumption of Richardson (1989). The load was monitored and the displacements were measured by gauge. American Society for Testing and Materials has established the basic procedure for conducting and calculation of PLI (ASTM D5731-08). The PLI for the diametral PLT is determined by the following equation (Broch and Franklin, 1972; ISRM, 2009):

$$PLI = P/d^2 \quad (1)$$

Where, P is failure load in N and d is core diameter in mm.

## 3. Numerical modeling

Finite element failure analysis was performed by using the ABAQUS program within the scope of this study. ABAQUS is capable of handling dedicated numerical models for the nonlinear response of concrete specimen under static and dynamic loading. Three constitutive models of concrete were provided in ABAQUS (Hibbitt et al., 2011): (1) brittle cracking (2) Smeared cracking and (3) damage plasticity. The concrete damage plasticity (CDP) model was used to simulate the mechanical behavior of concrete. The CDP model was used in numerical modeling which can determine both tensile and compressive behaviors of concrete where the tensile cracking and the compressive crushing, as two main failure mechanisms, can be investigated using this model.

Concerning CDP model in ABAQUS, the typical value range for dilation angle is between 30-40° according to (Jankowiak and àodygowski, 2005). The most satisfying results were obtained with 31°. To define α parameter, the ratio of biaxial compressive test to uniaxial tension stress was assumed to be equal to 1.16 as suggested by Kupfer et al. (1969). Typical value range for K is between 0.64-0.8 (Jankowiak and àodygowski, 2005; Lubliner et al. 1989) where the value of 0.67 was assumed for this study. The tensile strength of concrete was determined according to the equation provided in EN 1992-1-1 (1992). The elastic properties, elastic modulus and the poisson's ratio were calculated according to the procedure presented in EN 1992-1-1 (1992). Numerical results were compared with the experimental results of mix M1 at the age of 28 days. Three-dimensional (3D) hexahedral element, with 8 nodes and reduced integration C3D8R, was conducted using commercial finite element code ABAQUS. Due to the symmetry of specimen geometry, supports and loading conditions used in the PLT setup, only half of the specimen was modeled (Fig. 3). Loading and boundary conditions were applied as they were tested experimentally. The PLT were performed in closed-loop displacement control. The mesh used in the finite element analyses is shown in Fig. 4. The size of mesh is 0.7 mm in specimen.

## 4. Results and discussions

In PLT, specimens should fail by the development of one or more extensional planes containing the line of loading and these failure modes are referred to as valid failure modes, whereas deviation from these failure patterns is indicated as a failure in an invalid mode (ISRM, 2009). In this study, a unique failure mode was occasionally observed in concrete, where the specimen failed in two pieces as shown in Fig. 5. A view from the observation on the fracture formation of the specimen under PLT was detected that the specimen is accompanied by a failure along the plane containing the line of loading. It is note mentioning that the failure surface in the PLT is approximately in the middle of concrete specimen and perpendicular to the length of core, while the typical fracture pattern in cylindrical compressive strength test is diagonal and it is not exactly perpendicular to the length of core specimen (Del Viso et al., 2008).

The results of CS and PLI of various concrete mixes are given in Table 3. The CS test results were carried out on 100-mm cubes and PLT on core specimens with diameters of 50 and 70 mm with the ratio of L/D = 2. Figs. 6 and 7 present the development of the CS and PLI on concrete with various concrete mixes in different curing regimes at ages of 7, 14, 21, 28 and 42 days, respectively. It can be seen that the CS and PLI increased with concrete age for all concrete specimens. It was found that CS of concrete cured in water was higher than concrete under dry curing conditions. In general, CS of specimens increased on average about 8 % from dry to wet conditions. Also, as shown in Fig. 7, the PLI in wet curing conditions were about 12 % higher than those in dry curing conditions. It is noteworthy that this difference between wet and dry curing conditions for core diameter of 50 mm was close to that for core diameter of 70 mm, where the PLI for core diameters of 50 and 70 mm in wet curing conditions was found to be on average 13.5% and 11.15%, respectively, higher than that in dry curing conditions.

The standard deviation (SD) of CS and PLI is shown in Figs. 6 and 7. Concerning the age of 42 days, the mid-values of SD for CS in wet and dry curing conditions were found to be 0.91 and 1.12 MPa, respectively. As it is expected, the results in dry curing conditions were scattered more than those in wet curing conditions. Also, the mid-values of SD for PLI for core diameter of 50mm in wet and dry curing conditions were equal to 0.19 and 0.27 MPa, respectively, where the values of 0.08 and 0.13 MPa were obtained for core diameter of 70mm. The results show that the SD of PLI for core diameter of 50mm was more than that for core diameter of 70mm. Similar results were also reported by Rabins (1980), where the SD values can be affected by the size of specimens in PLT, and PLI values can be dissipated more by decreasing the core diameter of concrete specimen.

As shown in Fig. 6, under wet curing conditions, CSs of M2 in various ages were 82-86% higher than those of M1. These values were obtained between 85% and 91% under dry curing conditions. As indicated in Fig. 7, similar results were also attained in the PLT. For instance, under wet curing conditions, PLI values for M2 with core diameter of 50 mm increased between 48% and 60% compared to M1 where these values were obtained between 45% and 60% under dry curing conditions. These differences can be due to the fact that SF is a very finer compared to cement particles (each microsphere of SF is on average 100 times smaller than an average cement grain), which can cause SF to have more specific surface areas and subsequently react efficiently with water molecules. This manner can contribute to completing hydration process better and lead to obtaining CSs and PLI values for concrete specimens more (King, 2012).

Fig. 8 shows that for a given CS, there is a distinct difference between PLI of the specimen with wet and dry conditions. Based on Fig. 8, data from this study are fit to the power equation as suggested by Richardson (1989) in the form $CS = K\ (PLI)^n$. The correlation between CS and PLI is shown in Fig. 8. Richardson (1989) proposed, the coefficients of K and n are in the ranges of 6.68-15 and 1.18-1.85, respectively. As presented in Table 4, the results of this study show that both coefficients of K and n for all concrete specimens are in the ranges, detected by Richardson (1989). As indicated in Fig. 8, the difference between PLI values under wet and dry curing conditions for core diameter of 50 mm is more than that for core diameter of 70 mm. Similar results were also obtained by Robins (1980) where he concluded that for concrete specimens with certain CS, a reduction in core diameter will produce an increase in the PLI. It may be due to the fact that by considering a constant volume for core specimen, the surface area of core specimen increases by decreasing the core diameter which can lead to losing water content more. Therefore, for core specimens with lower core diameters, the differences between PLI values under wet and dry curing conditions increases.

The values of PLI gradually increased with a decrease in core diameter. The effect of core diameter on PLI has been clearly seen for concrete cores containing two different curing conditions. Generally, with the decrease in the concrete core diameter from 70 to 50 mm, PLI increased on average about 14% and 12% in wet and dry curing conditions, respectively. The effect of core diameter on PLI increased with age as shown in Fig. 9. Robins (1980) carried out a series of PLT on core specimen with the core diameters of 68 and 100 mm in order to investigate the effect of the size of specimen on PLI under wet curing conditions. As shown in Fig. 9(A), a comparison between the results, obtained by Robins (1980) for concrete specimen with core diameter of 68 mm, and the results of this study for concrete specimen with core diameter of 70 mm reveals that they are somewhat close to each other. However, a little difference between these two results can be due to the difference in the type and size of the aggregates.

By considering the fact that for each core diameter of 50 or 70 mm, there is a little difference between regression equations under wet and dry curing conditions (Fig. 8), Fig. 10 proposes some regression equations for core diameters of 50 and 70 mm which can be used in both wet and dry curing conditions.

Fig. 11 shows that the ratio of PLI/CS is dependent on curing conditions and CS of concrete where this ratio varies from 0.054 to 0.096 for core diameters of 50 and 70 mm. As shown in Fig. 11, the ratios of PLI/CS under dry curing conditions are higher than those under wet curing conditions.

The results showed that although both PLI and CS of concrete increase by increasing the age of concrete specimens (Fig. 7), the ratio of PLI/CS decreases when the level of strength increases (Fig. 11). This behavior shows that the rate of enhancement on CS of concrete is higher than that of PLI. This can be explained by the effect of destruction of drilling operation, where it weakens the bonds between the aggregate and the surrounding hardened cement paste. Also in high strength concrete, the bonds between cement paste matrix and aggregate are higher and more cohesive, so this will create more resistance during core operation and causes greater shearing between the coring bit and the concrete surface, which would cause greater damage to higher concrete strength. This finding is in agreement with various researchers. Selçuk and Gökçe (2015) reported that the ratio of the (PLI/CS) will decrease with the increase level of CS because the PLT is essentially a tensile test and the tensile failure in concrete occurs with a relatively small rate, compared to the concrete CS.

The load displacement responses were obtained from this numerical simulation and compared to the laboratory specimen results. The data from the FEM program is shown dotted line, whiles the product of the laboratory specimen is presented in a solid line. The resulting data are plotted in one graph and represents the specimens with 50 mm diameter for different L/D ratio in Fig. 12. As shown in Fig. 12, it can be seen that the proposed FEM produced a close approximation to the experimental curves.

As indicated in Fig. 13, the general shape of the curve obtained in present study is similar to that obtained by Robins (1980) where the vertical axis shows the ratio of PLI for various L/D ratios to PLI for L/D ratio of 2. The results demonstrates that the PLI increased particularly steep when the L/D ratio is less than 1, while then becomes less steep when the L/D ratio is between 1 and 1.8. Meanwhile, it seems that there is no significant difference among PLI values for the ratios of L/D more than 1.8. It can be inferred that only if the length of the core specimen increases, the dependence of PLI on total length of the specimen decreases. This behavior is also reported by Broch and Franklin (1972). In the experimental study by Robins (1980) suggested the minimum ratio of L/D to be 1.2 as shown in Fig. 13. Ishibashi et al. (2008) investigated the influence of L/D ratio of 0.5, 1, 1.5 and 2 on specific concrete grade, based on statistic analysis results. They stated that the core specimen with the ratio L/D less than 1 is not suitable to be examined by means of PLT. The reason is that core specimens had different frequency distribution and failure in imperfect.

To better understand the principal stress distribution along the direction of applying load, the two stresses $\sigma_z$ and $\sigma_y$ were obtained from the numerical modeling. The main directions of stresses, considered in numerical models, are shown in Fig. 14. $\sigma_z$ and $\sigma_y$ are normal stresses in the directions perpendicular and parallel, respectively, to the direction of applying load. The distribution of stresses along the line of loading for the specimen with L/D of 2 is shown in Fig. 15. As shown in Fig. 15, the distribution of stress $\sigma_z$ is tensile in more of loading line while distribution of stress $\sigma_y$ is compressive. The tensile stresses ($\sigma_z$) in the middle section are almost uniformly distributed; however, it increases sharply in the boundary regions between the tensile and compressive stresses. This may be attributed to the uncertainty, resulted from some plastic deformation beneath the load. However, the compressive stress ($\sigma_y$) is not uniformly distributed along the load diameter; they increase from the center of the diameter to the two loading points. $\sigma_y$ in the center of the specimen is about three times more than the magnitude of $\sigma_z$. The magnitude of the compressive stress at the contact points with platen is very high.

Al-Derbi and de Freitas (1999) stated that the maximum tensile stress at failure zone in PLT, determined by the Boussinesq equation, agrees well with the PLI value. They showed that there is a direct relationship between the maximum tensile stress and PLI. On the other hand, the results of present study indicated that there is a relationship between core diameter of concrete specimens and PLI (Fig. 9). In addition, as shown in Figs. 16 and 17, the maximum tensile stress of concrete specimen can be affected by the core diameter. A comparison between the results of the specimen with core diameter of 50 and 70 mm shows that the PLT failure can be expected to exhibit a size effect. The stress contours of the concrete specimens are shown In Figs. 16 and 17. All units are in (MPa). As shown in Fig. 16, there is the tensile stress normal to the failure plane in most places, but are accompanied by a compressive zone on the contact points of the conical platens and concrete specimens. It can be seen that the tensile stress has local distribution in the specimen under PLT, which occurs at some distance away from the two loading points. As shown in Fig. 16, maximum tensile stresses in the Z direction for specimens with core diameters of 50 and 70 mm are found to be roughly 2.32 MPa and 1.95 MPa, respectively. These values show that the maximum tensile stress for specimen with core diameter of 50 mm is 19 % more than that with core diameter of 70 mm. Similar results were also obtained by Al-Derbi and de Freitas (1999) where they concluded that the maximum tensile stress in specimen with lower core diameter is higher than that with larger core diameter. The stress in the Y direction is also shown in Fig. 17 where the maximum tensile stress for specimen with core diameter of 50 mm is 21 % more than that with core diameter of 70 mm. Generally, as expected, the tensile stresses in specimen increase as the core diameter decreases.

## 5. Conclusion

In this paper, the PLT was analyzed by means of experimental and FEM using ABAQUS software. The following conclusions can be drawn from this investigation:

- All data are indicative of the fact that numerical models can efficiently predict the fracture zone of core specimen in PLT similar to experimental observations. In addition, the correlation between CS and PLI is agreed well with the pervious correlation equations obtained by other researchers.
- In general, similar trend was found on improving PLI and CS with age. However, the ratio of PLI/CS decreases by increasing the level of strength which shows that the rate of enhancement of CS of concrete is higher than that of PLI.
- The results in this study show that PLI like CS is under the influence of curing conditions. The CS and PLI of the specimens under wet curing conditions were more than those under dry curing conditions.
- By decreasing core diameter from 70 to 50 mm, the PLI will increase by an average about 14% and 12% for core specimen in wet and dry curing conditions, respectively.
- According to the results of PLT on core specimens with different L/D ratios, the PLI increased with increasing L/D ratio. For L/D ratio less than 1, the increase in PLI was much greater than the increase in the range $1 \leq L/D \leq 1.8$. Meanwhile, it seems that there was no significant difference among PLI values for the ratios of L/D more than 1.8.
- For different core dimensions, although the values of stresses were not equal, similar stress distributions were detected on the failure surface. In addition, concrete specimens with smaller sizes had higher tensile strength compared to those with larger sizes.
- According to the numerical results, in Z direction, the maximum tensile stress for specimen with core diameter of 50 mm is 19 % more than that with core diameter of 70 mm. This value was found to be 21 % in Y direction.

## Conflict of Interest

The authors declare that there is no conflict of interest concerning this article.

## References


Al-Derbi, M.S. & de Freitas, M.H. (1999). Use of the Boussinesq Equation for determining the distribution of stress within a diametrical point load test. *Rock Mechanics and Rock Enineering,* 32(4), 257-265.

Bungey J.H., Millard S.G. & Grantham M.G. (2006). Testing of Concrete in Structures," *4th Edition, Taylor & Francis, London and New York,* 2006. 352p.

Broch, E. & Franklin, J.A. (1972). Point load strength test. *International Journal of Rock Mechanics and Mining Sciences,* 9(6), 669-697.

Chau, K.T. & Wei, X.X. (2001). A new analytic solution for the diametral point load strength test on finite solid circular cylinders. *International Journal of Solids and Structures*, 38(9), 1459-1481.

Del Viso J.R., Carmona J.R. & Ruiz G. (2008). Shape and size effects on the compressive strength of high-strength concrete. *Cement and Concrete Research,* 38(3), 386-395.

EN 1992-1-1. (1992). Eurocode 2. Design of concrete structures – Part 1-1: General rules and rules for buildings.

Hatheway, A.W. (2009). The complete ISRM Suggested methods for rock characterization, testing and monitoring; 1974–2006. *Environmental and Engineering Geoscience,* 15(1), 47-48.

Hibbitt, D. Karlsson, B. & Sorensen, P. (2011). ABAQUS Standard User's Manual. Version (6.11-3).

Ishibashi, K., Zacoeb, A. & Ito, Y. (2008). Influence of coarse aggregate size on the estimation of compressive strength of concrete by point load testing. *Journal of Structures and Materials in Civil Engineering,* 24: 108-115.

Jankowiak, T. & àodygowski, T. (2005). Identification of parameters of concrete damage plasticity constitutive model. *Foundations of Civil and Environmental Engineering*, 6, 53-69.

King D. (2012). The effect of silica fume on the properties of concrete as defined in concrete society report 74, cementitious materials. United Kingdom 37th Conference on Our World in Concrete & Structures, Singapore.

Kupfer, H., Hilsdorf, H. & Rusch, H. (1969). Behavior of concrete under biaxial stresses. *ACI Journal*, 66(8), 656-666.

Lubliner, J., Oliver, J., Oller, S. & Onate E. (1989). A plastic-damage model for concrete. *International Journal of Solids and Structures*, 25(3), 299-326.

Richardson, D.N. (1989). Point load test for estimating concrete compressive strength. *ACI Materials Journal,* 86(4), 409-416.

Robins, P.J. (1980). Point load strength test for concrete cores. *Magazine of Concrete Research*, 32(111), 101-111.

Russel, A.R. & Wood, D.M. (2009). Point load tests and strength measurements for brittle spheres. *International Journal of Rock Mechanics and Mining Sciences*, 46(2), 272-280.

Selçuk, L. & Süleyman Gökçe H. (2015). Estimation of the compressive strength of concrete under point load and its approach to strength criterions, *KSCE Journal of Civil Engineering*, 19(6), 1767-1774.

Wang, Y. (2005). Spatial variability of rock strength by irregular lump point load testing of welded topopah spring tuff, Ph.D. Thesis, University of Nevada, Reno. Wijk, G. (1980). The point load test for the tensile strength of rock. *Geotechnical Testing Journal*, 3(2), 49-54.

Zacoeb, A., Ishibashi, K. & Ito, Y. (2007). Estimating the compressive strength of drilled concrete cores by point load testing. *Proceeding of the 29th JCI Annual Meeting*, 525-530.

Zacoeb, A. & Ishibashi, K. (2009). Point load test application for estimating compressive strength of concrete structures from small core. *Journal of Engineering and Applied Sciences*, 4(7), 46-57.

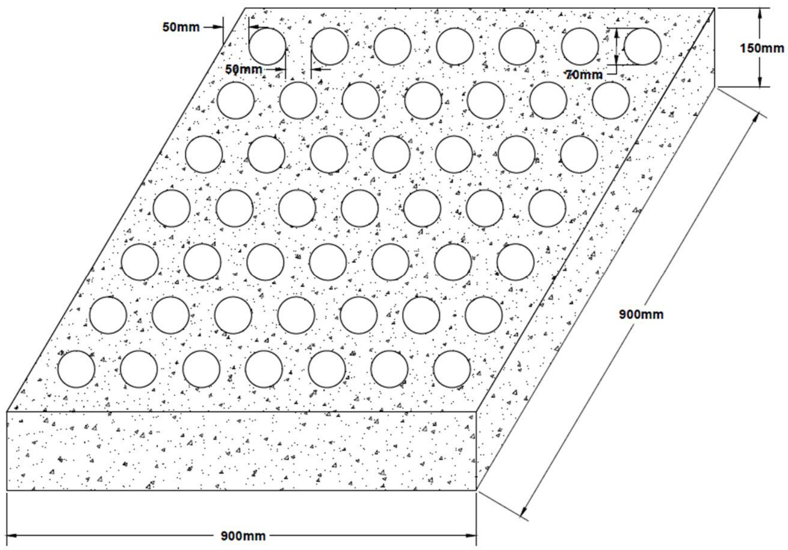


**Fig. 1.** Positions of core specimens in concrete slab.

(A) (B)

**Fig. 2.** (A) PLT machine and (B) configuration of specimen for PLT.

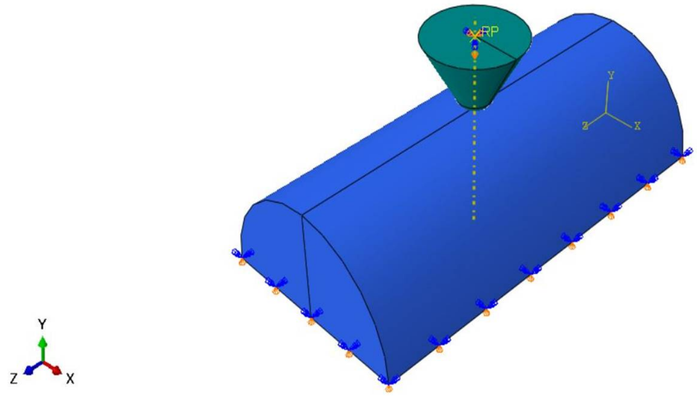


**Fig. 3.** Three-dimensional view of numerical model.

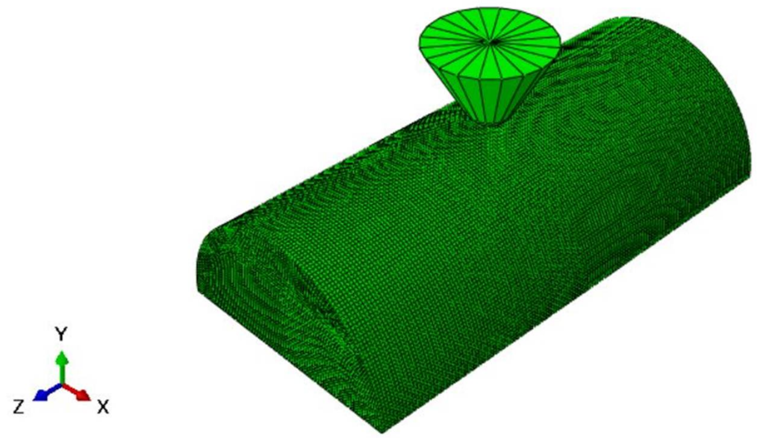


**Fig. 4.** Finite element mesh of the sample.


**Fig. 5.** A view of the concrete core sample under PLT.

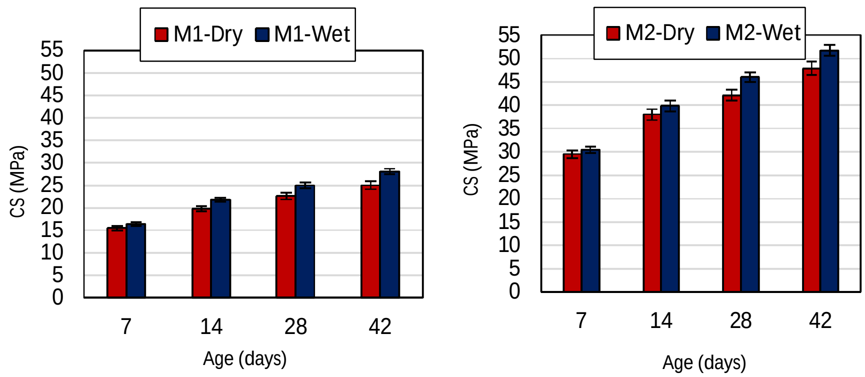


**Fig. 6.** Concrete CS gain with age in different curing conditions.

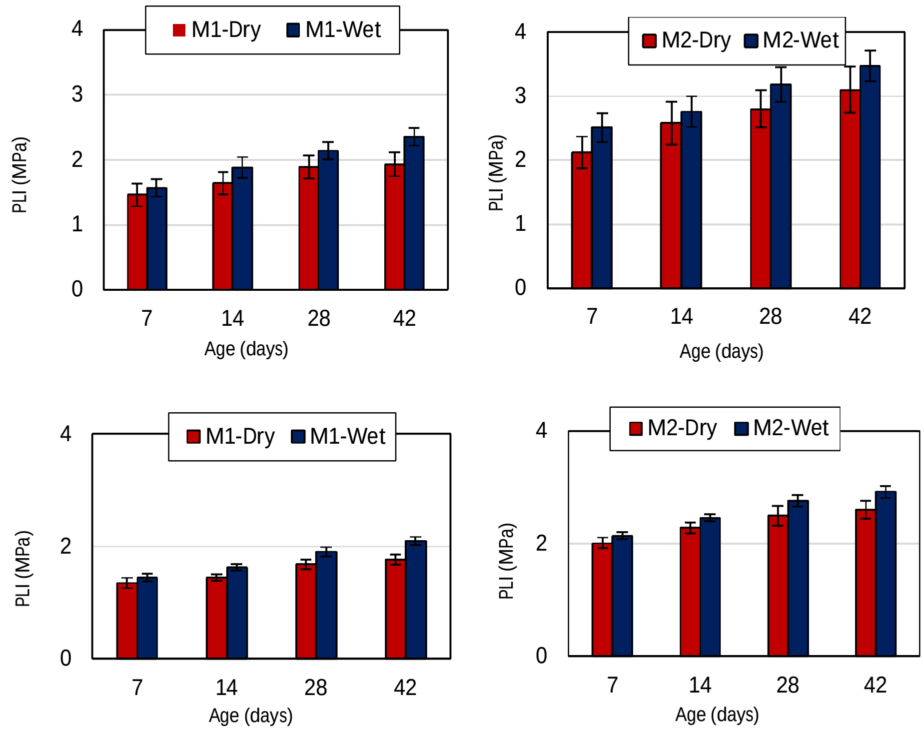


(A)

(B)

**Fig. 7.** PLI versus concrete age in different curing conditions in 50 mm (A) and 70 mm (B) core diameters.

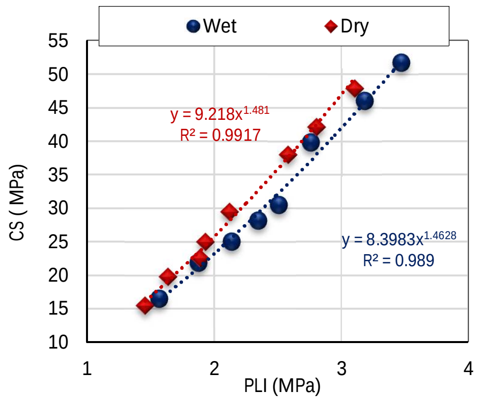


(A)

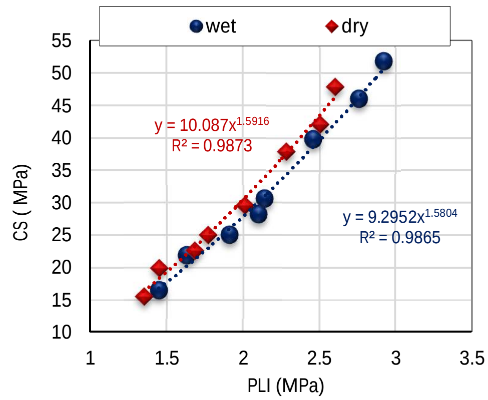


(B)

**Fig. 8.** Relationships between CS and PLI: (A) 50 mm and (B) 70 mm core diameters.

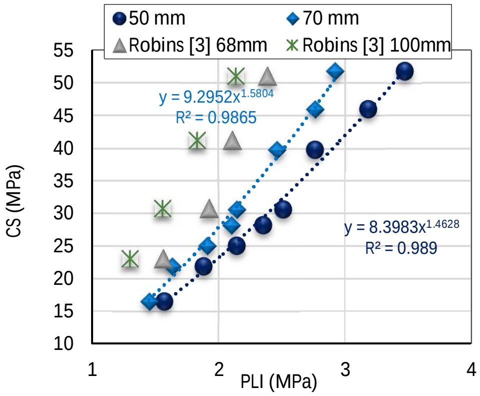


(A)

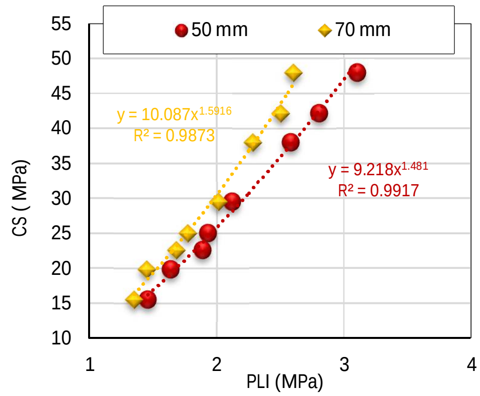


(B)

**Fig. 9.** Relationship between PLI and CS: wet (A) and dry (B) conditions.

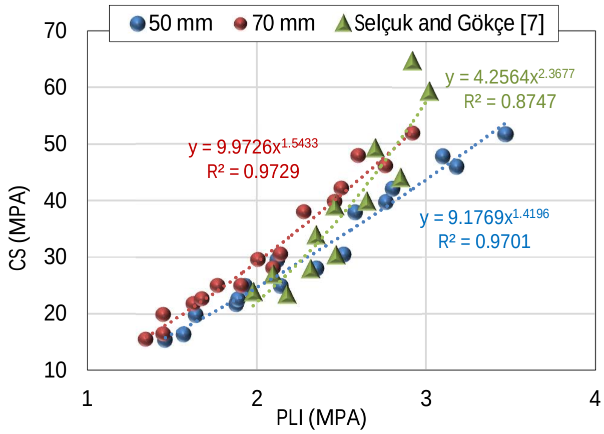


**Fig. 10.** Relationships between CS and PLI.

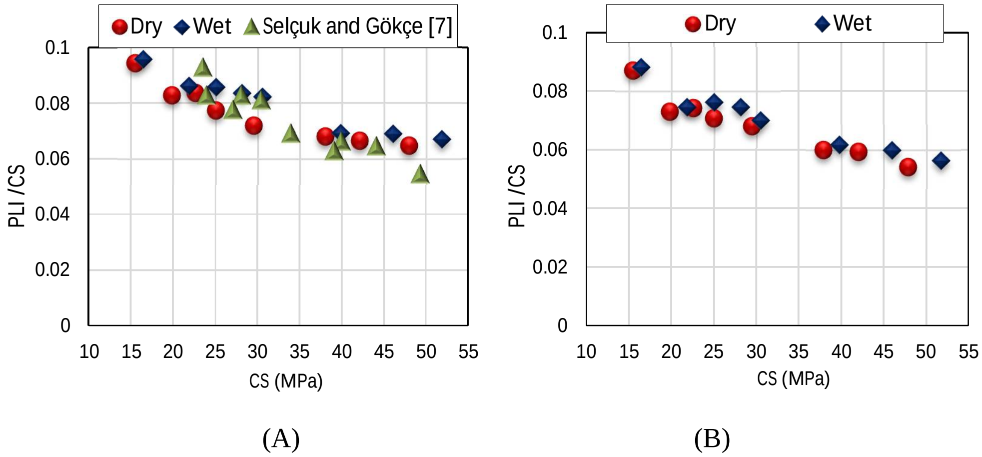


**Fig. 11.** Comparison of PLI/CS ratio for different curing conditions: 50 (A) and 70 mm (B) core diameters.

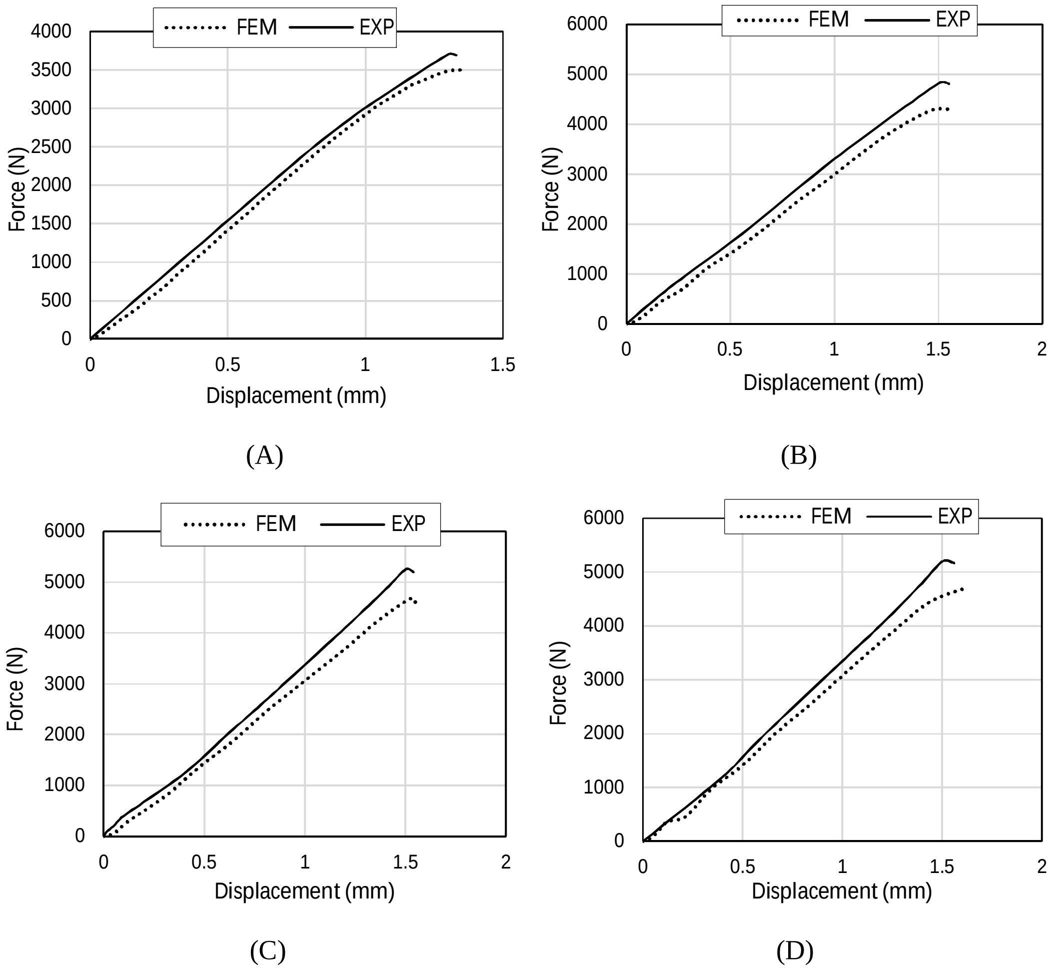


**Fig. 12.** Comparison of load- deflection curve with 0.5 (A), 1 (B), 2 (C) and 3 (D) L/D ratio.

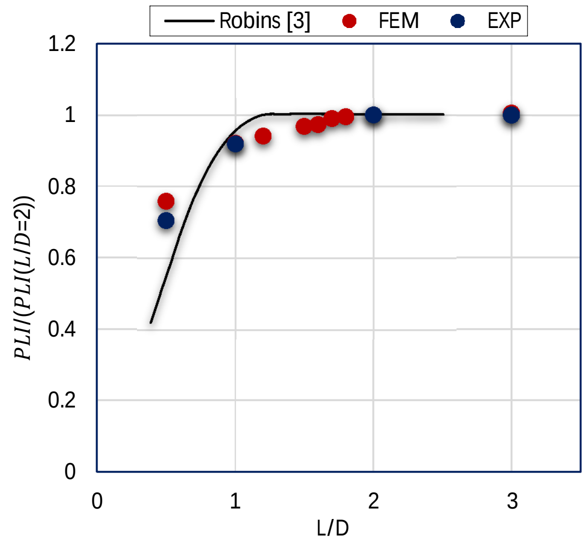


**Fig. 13.** The L/D ratio effect on PLI.

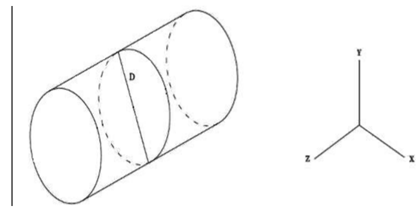


**Fig. 14.** The main directions of stresses considered in numerical models.

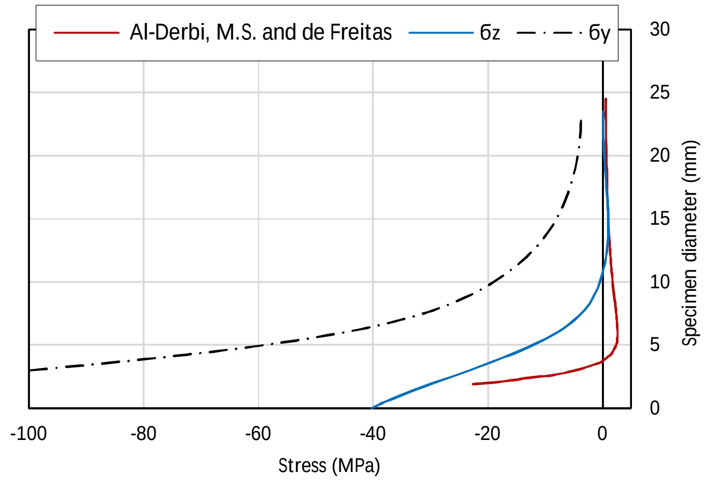


**Fig. 15.** Stress distribution along the load direction.

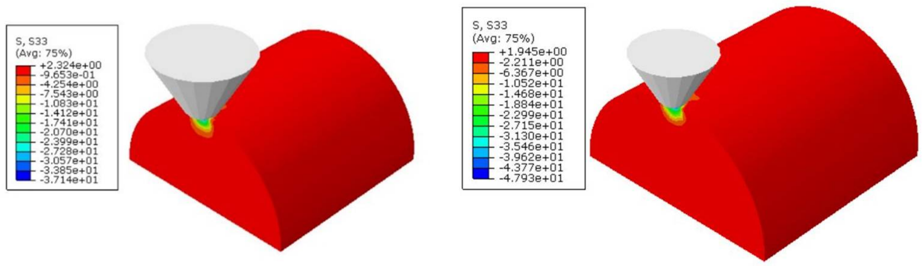


(A) (B)

**Fig. 16.** The distribution of stress in Z direction in the specimen: (A) D=50 mm and (B) D=70 mm.

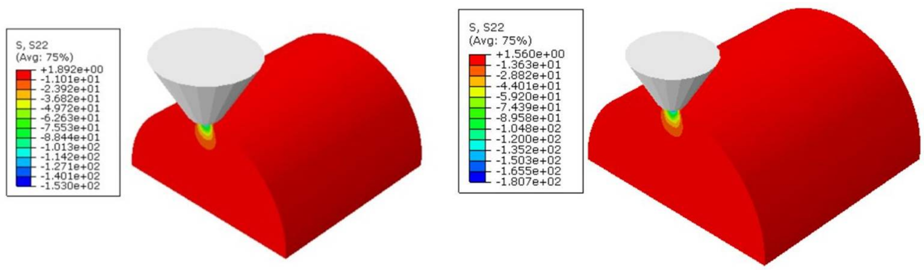


(A) (B)

**Fig. 17.** The distribution of stress in Y direction: (A) D=50 mm and (B) D=70 mm.